ISSN 1392–1320 MATERIALS SCIENCE (MEDŽIAGOTYRA). Vol. 10, No. 3. 2004

Dynamics of Au, Cu, Pt, Ni and Fe Nanoislands Growth on Amorphous Carbon

Gediminas JASINSKAS*, Arvaidas GALDIKAS

Department of Physics, Kaunas University of Technology, Studentų 50, LT-51368 Kaunas, Lithuania

Received 10 May 2004; accepted 08 July 2004

In this paper we present the fitting results of the experimental curves for the sputter deposition of Au, Cu, Pt, Ni and Fe on the amorphous carbon substrate. From the calculated curves the phenomenological coefficients which describe various steps (adsorption, adatom diffusion, cluster migration, coalescence) of deposition process are obtained. Considering different deposits the main influence have processes of nucleation of new clusters and adsorption at the edges of existing clusters. Discrimination of other processes (surface diffusion, cluster migration, coalescence) for different deposits is much less pronounced. It is shown for gold and copper the three-dimensional island growth mechanism, and for nickel and platinum two-dimensional island growth mechanism is prevailing. The cluster density depends on substrate temperature. The experimental results were obtained for Fe film deposition on amorphous carbon substrate at different target temperatures. The calculated results show that change of substrate temperature mainly influences not surface diffusion which could be expected but sticking of adatoms on substrate which drastically decreases with temperature increase.

Keywords: nanoclusters, island films, adsorption, surface diffusion, kinetic modeling.

INDEX

i_o – the relative flux of arriving atoms;
φ_S – the coverage by single adatoms;
φ_C – the coverage by islands;
n – the relative island density;
n_S – the relative density of adatoms;
λ – the diffusion radius of adatoms;
$\varphi_S^* = n_S\lambda^2 + 2\lambda\sqrt{n_S\varphi_S}$ – the dimensionless area around the single adatoms;
$\varphi_C^* = n\lambda^2 + 2\lambda\sqrt{n\varphi_C}$ – the dimensionless area around the clusters;
β – the migration radius of island;
φ_β – the dimensionless area around the island within the range of the migration radius of the island β;
α_{AA} – the probability of nucleation of the atoms, which are arriving at φ_S and φ_S*;
α_{A0} – the frequency probability of adatom to stick on the substrate surface;
α_{AC} – the frequency probability of adatom to stick at the edge of the island;
α_{AT} – the frequency probability of adatom to stick on the top of the island;
α_{col} – the frequency probability of coalescence.

INTRODUCTION

The growth of a solid film on a substrate generally takes place in one of the three modes (island, layer and island plus layer) which depend on the relative values of the adatom – adatom (cohesive) and adatom – substrate (adhesive) interaction energies. Certain deposition conditions, such as high vacuum, low supersaturation, high surface diffusion and lattice matching between the deposited film and the crystalline substrate, favour epitaxial layer growth. But where the epitaxial layer growth do not occur, as in the case of metals on alkali halides, MoS_2, MgO, SiO_2, mica and graphite, island growth predominates. When island growth does occur the nucleation density is profoundly affected by defects on the substrate surface because the adatom binding energy at a defect is greater than on the open surface.

Metal films may be deposited on substrates by a number of different techniques such as evaporation, sputtering, plasma decomposition etc. No matter which method is employed, it is necessary to have close control over the deposition parameters so that their individual influence on the growth processes can be observed. Ion beam sputtering (IBS), the technique used for preparing the samples studied in this paper, produces a well-defined flux of metal atoms sputtered by energetic inert gas atoms from a metal target surface. High-quality metal films may be fabricated owing to the energetic flux of metal atoms. Another major advantage of IBS is that the deposition rate is low and can be precisely controlled. The deposition can therefore be terminated at a very early stage in the substrate coverage, which allows initial stages of film growth to be observed [1].

Generally, five stages of film formation history may be considered in terms of the average cluster density and average cluster diameter [2 – 5]: 1) the induction time; 2) initial nucleation stage (both cluster density and size increases with time); 3) the saturation stage (cluster density has reached the maximum value, but the clusters continue to grow in size due to growth of adatoms to the clusters); 4) the coalescence stage (cluster density decreases rapidly); 5) the continuous growth stage.

Nucleation and islands growth are critical stages in thin film formation. Thus, a study of initial stages of thin film growth is fundamental to improve the understanding of growth mechanisms and to control the final materials microstructure, which governs the thin film properties [6].

*Corresponding author. Tel.: + 370-650-51640; fax: + 370-37-456472.
E-mail address: *gedasjas@yahoo.com* (G. Jasinskas)

The traditional view of epitaxial growth in the nucleation regime supposes that the process is initiated by binary collisions between adatoms that diffuse on the surface [7]. The resulting dimmer island nucleus may or may not be stable against dissociation before the arrival and attachment of further adatoms. So long as the adatom concentration on the surface exceeds its equilibrium value, an island population develops [8, 9]. In the classical theory of homogeneous nucleation it is assumed that all clusters of given size have only one, strictly determined shape. The cluster is usually approximated by that of spherical segment and by that of disk or prism of fixed height [10, 11]. According to the classical or capillary theory of nucleation the condensation of new phase of material takes place if the positive fluctuations of free energy needed for the existing activation barrier occurs [12]. Activation barrier is formed as a result of the changes in free energy with radius of cluster [13]. For a disk-shaped clusters free energy $F(i)$ (in units of kT) as a function of number of atoms in it i may be expressed as [14]

$$F(i) = 2\sqrt{ai} - i\ln(\xi + 1) - \ln\frac{n_0}{n_1} \qquad (1)$$

The first term in the eq. (1) describe surface tension, the second term describe the difference of chemical potential, and third is the statistical term related with the distribution of adatoms n, in the lattice surface nodal points n_0. The parameter a is expressed as $a = (\sigma/kT)^2\pi v/h$, where σ is the energy per unit length of disc boundary, v is the atomic volume in the cluster and h is the height of disc. The parameter ξ defines the oversaturation: $\xi = n_1/n_{1C} - 1$, where n_1 is the concentration of adatoms and n_{1C} is the concentration of adatoms at the thermodynamical equilibrium conditions.

In the early low-coverage stage two growth modes – a steady state and aggregation regimes are distinguished [15]. In the former, the growth process is dominated by evaporation from the surface and the diffusion of single atoms on the surface. The monomer concentration reaches a steady state and this governs the evolution of the islands. If evaporation from the surface is negligible, all atoms deposited diffuse and combine with existing islands. This regime is called as the aggregation regime.

The growth exponents and scaling behavior have been explored in details [15, 16, 17]. It was found the following time evolution of the main characteristic quantities at aggregation regime for three-dimensional islands the number of clusters N, the mean cluster size S and the surface coverage: $N \propto t^{1/7}$, $\langle S \rangle \propto t^{5/7}$, $M_1 \propto t^{5/7}$; and for two-dimensional islands: $N \propto \ln t$. $\langle S \rangle \propto t$, $M_1 \propto t$.

During film growth, islands are always growing because of deposition of material. In this early growth stage, when two islands touch, they quickly coalesce into a larger compact island, and in so doing wipe clean part of the substrate which was covered. This wiping action constantly creates gaps comparable to the island radius and results in overlarge islands separated by gaps filled with smaller islands nucleated since the lost wipe [18].

The random motion of islands on the substrate results in the so-called mobility coalescence [10, 19]. Mobility coalescence affects the cluster density time dependence, saturation cluster density, the cluster special distribution, cluster size distribution. The process of touching of two semi-spheres was studied in [20]. Below the bulk melting temperature and on scales smaller than 10 μm, the motion of atoms along the surface is the dominant mechanism for mass transport. Since large values of the surface curvature are concentrated around a very small region where the two spheres touch, one expects a very rapid local motion of the bridge joining the spheres. The mass flux is proportional to the gradient of surface curvature. The radius r which is defined as the height of bridge between two clusters exhibit power law scaling as a function of time and was found $r \propto t^{1/7}$.

In this work we use the partially improved model [21] which describes different modes of island-like growth of metal films. From the fitting of experimental curves the phenomenological coefficients which describe different steps of deposition process are found. Obtained values for different deposits and different deposition conditions are analyzed.

THE MODEL

1) ***Sticking coefficients.*** In order to consider layer-plus-island morphology of the growing film, four different sticking coefficients are introduced in model and surface coverages by single atoms $\varphi_S^{(1)}$ and clusters $\varphi_C^{(1)}$ are separated ($\varphi_S^{(1)} + \varphi_C^{(1)} = \varphi^{(1)}$).

Sticking of adatoms to the surface defines sticking coefficient α_{A0}. The surface coverage by islands increases when the arriving atom sticks at the edge of already existing island with probability α_{AC}. The sticking coefficient α_{AT} is the frequency probability of adatom to stick on the top of the island. The surface coverage by islands also increases when the arriving atom sticks at the already existing single adatom (island nucleation) with probability (or sticking coefficient) α_{AA} (Fig. 1).

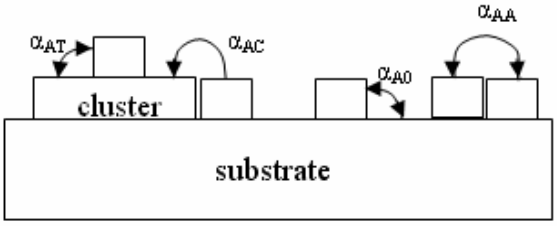

Fig. 1. Schematic of sticking coefficients

2) ***The diffusion radius of adatom.*** It is assumed in the model that island could capture adatom if it falls at the distance from the edge of the island less than λ (Fig. 2).

The dimensionless area φ_C* is obtained

$$\varphi_C^* = n\lambda^2 + 2\lambda\sqrt{n\varphi_C}$$

where n is the relative island density and λ is the diffusion radius of adatoms. The characteristic area around adatoms takes the following form

$$\varphi_S^* = n_S\lambda^2 + 2\lambda\sqrt{n_S\varphi_S}$$

where n_S is the relative density of adatoms.

Considering the growth of higher monolayers $K > 1$, the diffusion radius of the adatom on the top of island $\lambda_T^{(K)}$

is introduced. The parameter $\varphi_\lambda^{(K)}$ having meaning close to φ_C* is obtained as

$$\varphi_\lambda^{(K)} = 2 \cdot \lambda_T^{(K-1)} \sqrt{n\varphi^{(K-1)}} + n\left(\lambda_T^{(K-1)}\right)^2 .$$

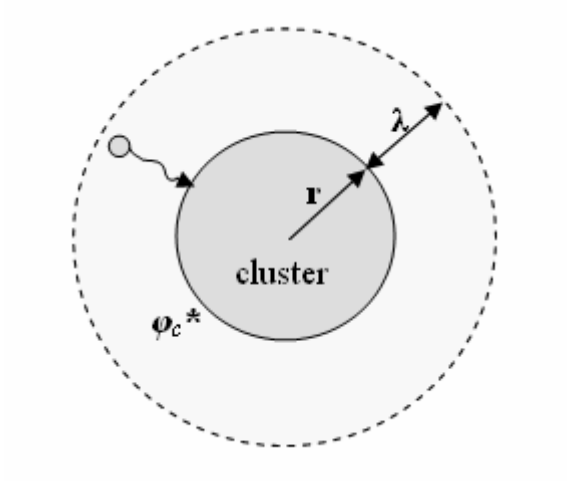

Fig. 2. Schematic definition of λ and φ_C*

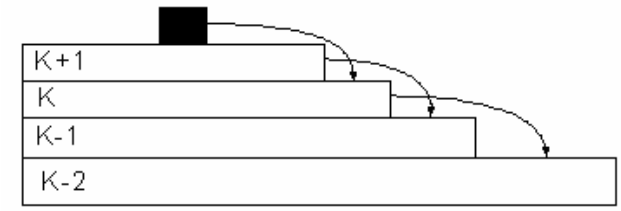

Fig. 3. The growth of higher monolayers ($K > 1$)

If $\varphi^{(K-1)} - \varphi^{(K)} \geq \varphi_\lambda^{(K)}$ then the adatoms stick on the $(K–1)^{\text{th}}$ monolayer and form K^{th} monolayer; and if $\varphi^{(K-1)} - \varphi^{(K)} < \varphi_\lambda^{(K)}$ then the adatoms move to $(K–2)^{\text{th}}$ monolayer and form $(K–1)^{\text{th}}$ monolayer (Fig. 3).

The equation for the coverage of K^{th} monolayer in our model is the following:

$$\frac{d\varphi^{(K)}}{dt} = A^{(K)}\alpha_{AT} i_0 \left(\varphi^{(K-1)} - \varphi^{(K)}\right) +$$
$$+ B^{(K)}\alpha_{AT} i_0 \left(\varphi^{(K)} - \varphi^{(K+1)}\right)\left(\varphi^{(K-1)} - \varphi^{(K)}\right), \quad K = 2,3,...,N$$

The coefficients $A^{(K)}$ and $B^{(K)}$ are introduced from the condition $\varphi^{(K)} \leq 1$:

$$A^{(K)} = \begin{cases} 0 & \text{if} \quad \varphi^{(K-1)} - \varphi^{(K)} < \varphi_\lambda^{(K)} \\ 1 & \text{if} \quad \varphi^{(K-1)} - \varphi^{(K)} \geq \varphi_\lambda^{(K)} \end{cases}$$
$$K = 2,3,...,N$$

$$B^{(K)} = \begin{cases} 0 & \text{if} \quad \varphi^{(K)} - \varphi^{(K+1)} \geq \varphi_\lambda^{(K)} \\ 1 & \text{if} \quad \varphi^{(K)} - \varphi^{(K+1)} < \varphi_\lambda^{(K)} \end{cases}$$
$$K = 1,2,...,N$$

3) ***Nucleation.*** The atoms arriving at φ_S and φ_S*, nucleate with probability α_{AA}. The nucleation term may be expressed as $nucl = \alpha_{AA} i_0 \left(\varphi_S + \varphi_S^*\right)$. The increase in number of islands per unit time is $\frac{dN_C}{dt} = \frac{nucl}{2\varphi_a}$, where φ_a is the area of one atom (dimensionless) multiplied by factor of 2 because two stuck atoms become as one island; then:

$$\left(\frac{dn}{dt}\right)_n = \frac{1}{2}\alpha_{AA} i_0 \left(\varphi_S + \varphi_S^*\right).$$

4) ***The migration radius of the island β and the coalescence effect.*** Value φ_β is the dimensionless area around the island within the range of the migration radius of the island β (Fig. 4). φ_β may be obtained in the same way as φ_C* or φ_S* and is expressed as $\varphi_\beta = n\beta^2 + 2\beta\sqrt{n\varphi_C}$.

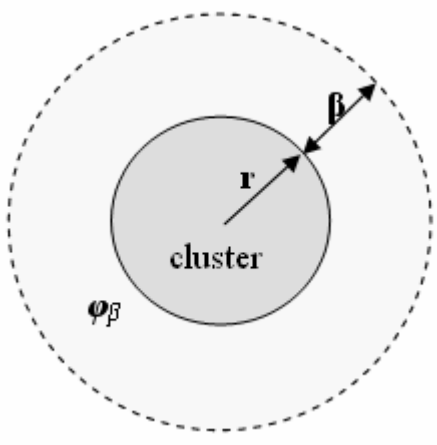

Fig. 4. Schematic definition of β and φ_β

During film growth, islands are always growing because of deposition of material. In this early growth stage, when two islands touch, they quickly coalesce into a larger compact island, and in so doing wipe clean part of the substrate which was covered (Fig. 5).

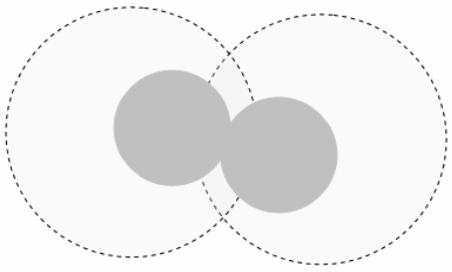

Fig. 5. The mobility coalescence effect

The term of mobility coalescence may be obtained from the assumption that coalescence occurs when $\varphi_C + \varphi_\beta \geq 1$. The coalescence term is

$$\left(\frac{dn}{dt}\right)_C = \alpha_{col} C_{col} \left(1 - \varphi_C - \varphi_\beta\right),$$

where C_{col} is normalization factor that may obtain two values:

$$C_{col} = \begin{cases} 0 \text{ if } \varphi_C + \varphi_\beta < 1 \\ 1 \text{ if } \varphi_C + \varphi_\beta \geq 1 \end{cases}$$

The coefficient α_{col} is the frequency probability of coalescence (s^{-1}). During deposition the surface coverage increases $\left(\varphi_S + \varphi_C\right) \to 1$ and it means that the areas φ_S*

and φ_C* decrease. Fulfilling the following condition $\varphi_L \le 1$, where $\varphi_L = \varphi_S + a(t)\varphi_S^* + \varphi_C + a(t)\varphi_C^*$, the normalization parameter a(t) is introduced which obtain the following values

$$a(t) = \begin{cases} 1 & \text{if} \quad \varphi_L < 1 \\ \dfrac{1-\varphi_S(t)-\varphi_C(t)}{\varphi_S^*(t)+\varphi_C^*(t)} & \text{if} \quad \varphi_L \ge 1 \end{cases}.$$

All steps of deposition process can be expressed as the following system of equations:

$$\begin{cases} \dfrac{d\varphi_S}{dt} = \alpha_{A0} i_0 (1-\varphi_L) - \alpha_{AA} i_0 \left(\varphi_S + a(t)\varphi_S^*\right) \\ \dfrac{d\varphi_C}{dt} = 2 \cdot \alpha_{AA} i_0 \left(\varphi_S + a(t)\varphi_S^*\right) + a(t)\alpha_{AC} i_0 \varphi_C^* + \\ + B^{(1)} \alpha_{AC} i_0 \left(1-\varphi^{(1)}\right)\left(\varphi^{(1)} - \varphi^{(2)}\right) \\ \dfrac{d\varphi^{(K)}}{dt} = A^{(K)} \alpha_{AT} i_0 \left(\varphi^{(K-1)} - \varphi^{(K)}\right) + \\ + B^{(K)} \alpha_{AT} i_0 \left(\varphi^{(K)} - \varphi^{(K+1)}\right)\left(\varphi^{(K-1)} - \varphi^{(K)}\right), \\ \qquad\qquad K = 2,3,\ldots,N \\ \dfrac{dn}{dt} = \dfrac{1}{2} \cdot \alpha_{AA} i_0 \left(\varphi_S + a(t)\varphi_S^*\right) + \alpha_{col} C_{col} \left(1-\varphi_C - \varphi_\beta\right) \end{cases} \quad (2)$$

RESULTS AND DISCUSSIONS

In Fig. 6 (a) – (f) the kinetics of surface coverage $\varphi^{(1)}(t)$ and average cluster size (diameter) are presented. The calculated results (solid lines) are compared with experimental ones (points) obtained by S. Xu and B. L. Evans [1, 22] for Au, Cu, Ni and Pt deposition on amorphous carbon substrate. The calculated curves for different deposits (Au, Cu, Ni and Pt) have been obtained at different values of two parameters: α_{A0} and α_{AC}. Values are summarized in Table 1.

Table 1. The values of parameters α_{A0}, α_{AC} and α_{AT} for different deposits

	Au	Cu	Ni	Pt
α_{A0}	0.17	0.1	0.9	0.152
α_{AC}	11	8.8	100	147.8
α_{AT}	1	1	1	1

Other parameters have been kept the same (they are indicated in legend of figures). For all deposits $\alpha_{A0} < \alpha_{AC}$, and the α_{AC} values for platinum and nickel are much more higher than the α_{AC} values for copper and gold. The α_{AO} values are very similar for platinum, gold and copper; and the nickel has a little bit higher α_{A0} value than other three mentioned deposits. If $\alpha_{A0}/\alpha_{AC} < 1$, the growth by islands occurs. Island growth for nickel ($\alpha_{A0}/\alpha_{AC} = 0.009$) and platinum ($\alpha_{A0}/\alpha_{AC} \approx 0.001$) is more pronounced than for other two deposits – gold ($\alpha_{A0}/\alpha_{AC} \approx 0.015$) and copper ($\alpha_{A0}/\alpha_{AC} \approx 0.011$). At the higher values of the ratio α_{AT}/α_{AC} the islands three-dimensional growth is more presumptive. For gold ($\alpha_{AT}/\alpha_{AC} \approx 0.091$) and for copper ($\alpha_{AT}/\alpha_{AC} \approx 0.114$) three-dimensional island growth is much more pronounced than for other two deposits: platinum ($\alpha_{AT}/\alpha_{AC} \approx 0.007$) and nickel ($\alpha_{AT}/\alpha_{AC} = 0.01$). It is likely, that for nickel and platinum island growth is two-dimensional, and for gold and copper island growth is three-dimensional.

It is interesting to analyze and compare results obtained by different authors in different laboratories for the same deposits on the same substrates. Such analysis was made and calculated results are presented in Fig. 6 (g) – (h) and are compared with experimental ones for sputter deposition of gold on the amorphous carbon substrate with the deposition rate of $1.2 \cdot 10^{14}$ cm^{-2}s^{-1} at room temperature and at $5 \cdot 10^{-3}$ Pa pressure [23].

If compare Fig. 6 (a), (b) with Fig. 6 (g), (h) it is seen that the majority of coefficients for two cases of Au deposition on amorphous carbon are the same or very similar, but the values of three coefficients (α_{AA}, α_{AC} and λ) particularly differ. The reason of such mismatch might be different conditions of deposition of Au thin films.

In the case of Fig. 6 (g), (h) depositions were performed using a Kaufmann ion source operating at 1200 V. The pressure was 5×10^{-5} Pa prior deposition and 5×10^{-3} Pa during deposition when Ar gas was admitted to the ion source. The angle between the axis of the ion beam and the normal to the target was 45°. The substrate holder was parallel to the target at a distance equal to 10 cm. All depositions were made at room temperature and the substrate holder was water cooled to prevent possible heating [23]. In the case of Fig. 6 (a), (b) the deposition chamber was cryopumped to a pressure of less than 5×10^{-5} Pa. When high-purity Ar gas was admitted to the ion gun, the dynamic Ar gas pressure within the continuously pumped chamber increased to 6.6×10^{-2} Pa. A d.c. voltage was applied to the ion gun to initiate the discharge and the Ar gas supply adjusted (and subsequently computer-regulated) to give the required value of ion gun voltage (during the deposition of Au thin films voltage was 2200 V). The flux of inert gas ions and excited atoms from the ion gun was incident on the target at an angle of 60° to the normal [22]. Different conditions of Au deposition in the cases of Fig. 6 (a), (b) and Fig. 6 (g), (h) might determine the different energies of atoms falling from the target to substrate. The different energies of atoms arriving to substrate are the most reliable reason to explain the high differences between three mentioned coefficients (α_{AA}, α_{AC} and λ).

Above different deposits were analyzed. For detailed analysis it is necessary to consider results for the same deposit at different deposition conditions. In Fig. 7 the experimental results (points) obtained by X. X. Zhang and E. Y. Jiang [24] for Fe film depositions on amorphous carbon substrate at different target temperatures are presented. As the flux of Fe atoms was 10^{12} cm^{-2}s^{-1} these results represents the initial stages of film growth. The fitting show that not diffusion but sticking process is mainly influenced by temperature changes. By variation of parameter λ a good fit was not obtained [21]. The best fit was done by decreasing parameter α_{A0} with increase of temperature. Other parameters have been kept as constants.

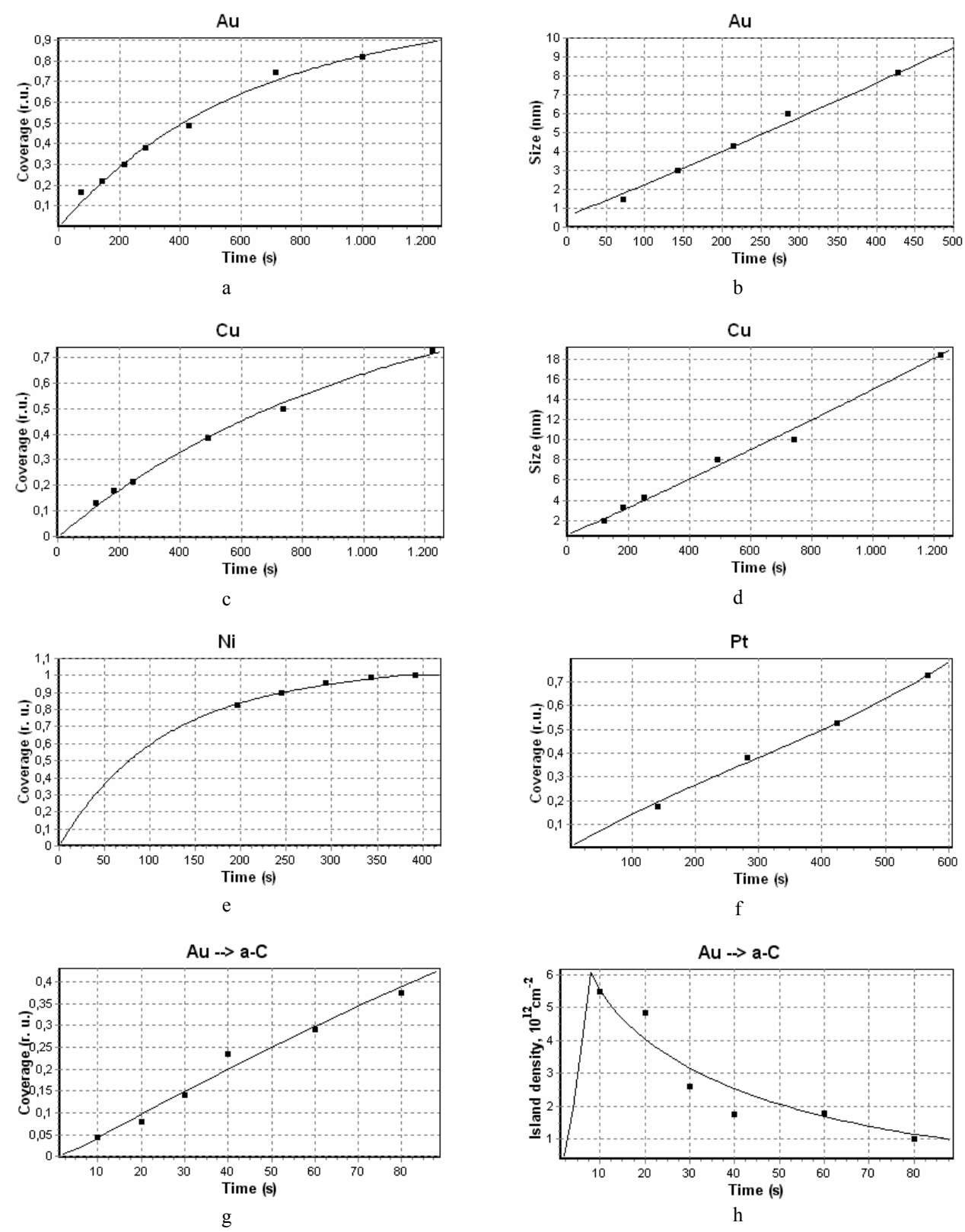

Fig. 6. The time dependences of surface coverage for four different deposits: a – Au, c – Cu, e – Ni, f – Pt; the time dependences of average cluster size for two different deposits: b – Au, d – Cu. The calculated curves are obtained from equations (2) at the following values of parameters, which are the same for all deposits: $\alpha_{AA} = 10^{-6}$; $\alpha_{AT} = 1$; $\alpha_{col} = 1$; $\beta = 35$; $\lambda = 1$; $\lambda_T = 30$; $i_0 = 0.01$. Values of other two parameters are different for different deposits and are shown in Table 1. Experimental results are taken from ref. [1, 22]. g – h: g – the calculated kinetics (line) of first monolayer coverage; h – the calculated kinetics (line) of island density. Experimental results (squares) are for sputter deposition of gold on amorphous carbon. Calculation parameters are the same for the both presented figures: $\alpha_{A0} = 0.19$; $\alpha_{AA} = 1.1$; $\alpha_{AC} = 0.323$; $\alpha_{AT} = 1$; $\alpha_{col} = 1$; $\beta = 35$; $\lambda = 37$; $\lambda_T = 30$; $i_0 = 0.01579$. Experimental results are taken from ref. [23]

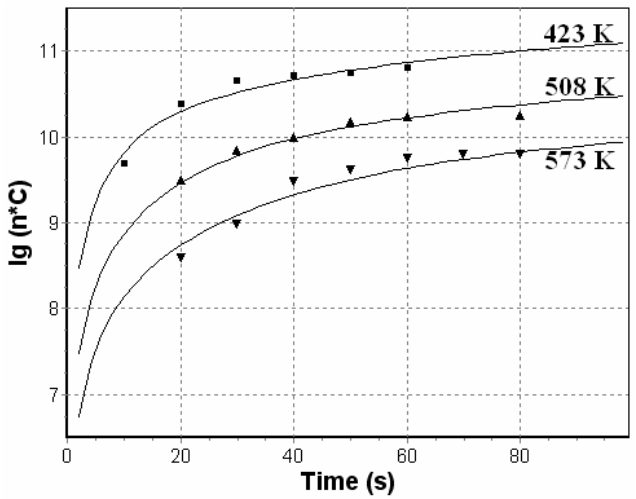

Fig. 7. Logarithmic plot of the time dependences of cluster density for different substrate temperatures: $T = 423$ K – $\alpha_{A0} = 0.3$; $T = 508$ K – $\alpha_{A0} = 0.03$; $T = 573$K – $\alpha_{A0} = 0.0055$. Other parameters are the same for all temperatures: $\alpha_{AA} = 10^{-5}$; $\alpha_{AT} = 1$; $\alpha_{AC} = 1$; $\alpha_{col} = 1$; $\beta = 1$; $\lambda = 350$; $\lambda_T = 1$; $i_o = 0.1$; $C = 10^{16}$ cm^{-2}. Experimental points obtained for Fe deposition on amorphous carbon substrate at flux density 10^{12} cm^{-2}s^{-1} at different substrate temperatures, taken from ref. [24]

CONCLUSIONS

1. For Au and Cu 3-D and for Pt and Ni 2-D island growth mode is prevailing because of different sticking of adatoms on the top and at the edge of islands.
2. The main differences of deposition at the same conditions of different deposits are: 1) sticking on the surface and 2) sticking at the edge. Other steps of deposition process are similar.
3. Analyzing deposition of the same deposits is concluded that energy of arriving atoms mainly influences the following processes: 1) surface diffusion, 2) nucleation and 3) sticking at the edge.
4. Considering very beginning of deposition process is concluded that change of substrate temperature mainly influences not surface diffusion which could be expected but sticking of adatoms on substrate which decreases with temperature increase.

REFERENCES:

1. **Shi Xu, Evans, B. L., Flynn, D. I., Cao En.** The Study of Island Growth of Ion Beam Sputtered Metal Films by Digital Image Processing *Thin Solid Films* 238 1994: pp. 54 – 61.
2. **Anton, R., Schmidt, A. A.** Anomalous Nucleation and Growth of Metal and Alloy Particles During Vapor Deposition on Amorphous Substrates *Surface Science* 357 – 358 1996: pp. 835 – 839.
3. **Zhang, X. B., Vasiliev, A. L., Van Tendeloo, G., Yan He, Yu, L.–M., Thiry, P. A.** EM, XPS and LEED Study of Deposition of Ag on Hydrogenated Si Substrate Prepared by Wet Chemical Treatments *Surface Science* 340 1995: pp. 317 – 327.
4. **Ernst, H. J., Fabre, F., Lapujoulade, J.** Nucleation and Diffusion of Cu Adatoms on Cu(100): A Helium-Atom-Beam Scattering Study *Phys. Rev. B* 46 (3) 1992: pp. 1929 – 1932.
5. **Jensen, P., Combe, N.** Understanding the Growth of Nanocluster Films *Computational Materials Science* 24 2002: pp. 78 – 87.
6. **Andreazza, P., Andreazza-Vignolle, C., Rozenbaum, J. P., Thomann, A.-L., Brault, P.** Nucleation and Initial Growth of Platinum Islands by Plasma Sputter Deposition *Surface and Coatings Technology* 151 – 152 2002: pp. 122 – 127.
7. **Fedoseev, D. V., Chyzhko, R. K., Gribcov, A. G.** Heterogeneous Crystallization from Gaseous Dose. Moscow: Nauka, 1978 (in Russian).
8. **Zangwill, A., Kaxiras, E.** Submonolayer Island Growth with Adatom Exchange *Surface Science* 326 1995: pp. L483 – L488.
9. **Riveros, H., Cabrera, E., Gally, M., Ruiz – Mejia, C., Fujioka, J.** Models for the Early Stages of Nucleation *Journal of Crystal Growth* 128 1993: pp. 44 – 49.
10. **Stoyanov, S., Kashchiev, D.,** in ed. by **Kaldis E.** Topics in Materials Science. Vol. 7. North-Holland Pub. Comp., 1981.
11. **Yu, G., Lai, J. K. L.** Kinetics of Transformation with Nucleation and Growth Mechanism: Two- and Three-Dimensional Models *Journal of Applied Physics* 79 (7) 1996: pp. 3504 – 3511.
12. **Osipov, A. V.** Kinetic Model of Vapour-Deposited Thin Film Condensation: Nucleation Stage *Thin Solid Films* 227 1993: pp. 111 – 118.
13. **Oh, Ch. W., Kim, E., Lee, Y. H.** Kinetic Role of a Surfactant in Island Formation *Phys. Rev. Lett.* 76 (5) 1996: pp. 776 – 779.
14. **Kukushkin, S. A., Osipov, A. V.** Thin Film Condensation Processes *Physics - Uspekhi* 168 (10) 1998: pp. 1083 – 1116 (in Russian).
15. **Family, F., Popescu, M. N., Amar, J. G.** Self-Consistent Rate Equation Theory of Cluster Size Distribution in Aggregation Phenomena *Physica A* 306 2002: pp. 129 – 139.
16. **Blackman, J. A.** Growth Models for Discontinuous Films *Physica A* 220 1995: pp. 85 – 98.
17. **Bartelt, M. C., Evans, J. W.** Scaling Analysis of Diffusion-Mediated Island Growth in Surface Adsorption Processes *Phys. Rev. B* 46 (19) 1992: pp. 12675 – 12687.
18. **Yu, X., Duxbury, P. M., Jeffers, G., Dubson, M. A.** Coalescence and Percolation in Thin Metal Films *Phys. Rev. B* 44 (23) 1991: pp. 13163 – 13166.
19. **Geguzin, J. E.** Diffusive Processes on the Crystal Surface. Moscow: Energoatomizdat, 1984 (in Russian).
20. **Eggers, J.** Coalescence of Spheres by Surface Diffusion *Phys. Rev. Lett.* 80 (12) 1998: pp. 2634 – 2637.
21. **Galdikas, A.** Thin Film Deposition onto the Rough Surface: Phenomenological Investigations *Thin Solid Films* 418 2002: pp. 112 – 118.
22. **Shi Xu, Evans, B. L.** Nucleation and Growth of Ion Beam Sputtered Metal Films *Journal of Materials Science* 27 1992: pp. 3108 – 3117.
23. **Muzard, S., Templier, C., Delafond, J., Girard, J. C., Thiaudiere, D., Pranevicius, L., Galdikas, A.** Development of the Microstructure of Sputter Deposited Gold on Amorphous Carbon *Surface and Coatings Technology* 100 – 101 1998: pp. 98 – 102.
24. **Zhang, X. X., Jiang, E. Y.** The Nucleation and Initial Growth of Iron Films Deposited by Facing Targets Sputtering *Journal of Magnetism and Magnetic Materials* 121 1993: pp. 46 – 48.